SUBSURFACE CHARACTERIZATION USING SYNCHROSQUEEZING TRANSFORM WITH HIGH-ORDER APPROXIMATIONS

HUI LV

School of Civil Engineering and Architecture, Nanchang Hangkong University, 696 South Fenghe Avenue, Nanchang 330063, P.R. China. lv_hui2016@126.com

(Received August 9, 2018; revised version accepted October 5, 2019)

ABSTRACT

Lv, H., 2020. Subsurface characterization using synchrosqueezing transform with high-order approximations. *Journal of Seismic Exploration*, 29: 1-14.

Time-frequency analysis methods always play an important role in subsurface seismic characterization. Due to the advantages in characterizing non-stationary signals, time-frequency analysis often obtains higher resolution than the competing methods. In this paper, we present a novel technique for subsurface seismic characterization based on a synchrosqueezing transform with high-order approximation. The new synchrosqueezing transform can obtain more accurate instantaneous frequencies by using the higher order approximations for both amplitude and phase in order to achieve a highly energy-concentrated time-frequency representation. We use a synthetic example to demonstrate an excellent time-frequency representation using the proposed method, i.e., to extract the time-frequency variation relation. Applications of the proposed method on two field data sets demonstrate the potential of the new method in detecting low-frequency anomaly and detecting paleo-channels with a higher time-frequency resolution. These two geological features are crucial for subsurface characterization since they are usually related with oil & gas.

KEY WORDS: subsurface characterization, seismic signal processing, time-frequency analysis.

0963-0651/20/$5.00

INTRODUCTION

Time-frequency analysis has been gaining importance in seismic processing and interpretation over the past few years because it is capable of providing considerable information that includes the subsurface rocks and reservoirs (Gan et al., 2016c; Chen and Song, 2018; Liu et al., 2017b; Wang et al., 2018b; Zhang et al., 2018). Time-frequency (TF) analysis solves the problems of identifying and quantifying the oscillatory components presented in the signal, which has been exclusively utilized by the field of exploration geophysics over the past two decades (Partyka et al., 1998; Castagna et al., 2003; Chen et al., 2016c,b; Zu et al., 2016, 2017; Chen et al., 2017e; Siahsar et al., 2017a; Chen, 2017; Siahsar et al., 2017b,c).

Commonly used approaches for time-frequency analysis are typically short-time Fourier transform (STFT) (Allen, 1977) and continuous wavelet transform (CWT) (Sinha et al., 2005; Chen et al., 2014a; Liu et al., 2016a). However, both of them share the same limitation, known as the ”Heisenberg uncertainty principle”, stipulating that one cannot simultaneously accomplish the best time and frequency resolutions (Liu et al., 2016b). Several attempts were made to overcome this issue, as for instance the reassignment method (RM). The main shortcoming with respect to RM is its non invertibility, which directly results in the difficulty for recovering the original signal. The empirical mode decomposition (EMD) (Huang et al., 1998; Chen, 2016; Chen et al., 2017b) algorithm can separate a signal into locally-constant frequency components, and have been shown to have a high resolution both in time and frequency with some types of extensions, like ensemble empirical mode decomposition (EEMD) (Chen et al., 2017d) and complete ensemble empirical mode de- composition (CEEMD) (Chen et al., 2016a, 2017a). However, the EMD algorithm is still remaining heuristic because of the lack of mathematical support.

Subsequently Daubechies et al. (2011) introduced an adaptive signal analysis tool, called sychrosqueezing transform (SST) which originally derives from the field of audio signal, it aims at improving the time-scale representation resulted from CWT and allowing for mode reconstruction (Chen et al., 2014b; Liu et al., 2016d). Inspired by SST, Thakur and Wu (2011) proposed an extension of SST to the time-frequency representation given by STFT, namely STFT-based SST. Despite its remarkable success in enhancing time-frequency resolution, there are still some disadvantages associated with its use, especially in dealing with these signals with “fast varying” instantaneous frequency (Liu et al., 2017a). Recently, some work has been done on how to combat this problem. Oberlin et al. (2015) introduced an adaptation of the STFT-based SST to better cope with this case, known as the second order synchrosqueezing transform, which achieves a compact time-frequency representation while allowing for mode retrieval. An alternative technique, called the high-order synchrosqueezing transform was proposed by Pham and Meignen (2017), which is a new

generalization of the STFT-based synchrosqueezing transform to compute more accurate estimates of the instantaneous frequencies.

Time-frequency analysis methods can also be used for suppression random noise in seismic data (Gan et al., 2015, 2016a; Li et al., 2016a,b; Gan et al., 2016b; Chen et al., 2017c; Zhou et al., 2017; Wang et al., 2018a; Zhou et al., 2018; Chen and Fomel, 2018). The time- frequency peak filtering based methods proposed by Roessgen and Boashash (1994) encode the analyzed seismic signal as the instantaneous frequency (IF) of an analytic signal. Then, the TFPF based methods apply the Wigner-Ville distribution (WVD) (Jeffrey and William, 1999) to estimate the IF of the analytic signal and suppress seismic random noise. Lin et al. (2015) combined the matching pursuit and time-frequency digital filtering method based on an invertible wavelet transform and applied it to evoked potentials. Liu et al. (2013) introduced the pseudo-WVD (PWVD) instead of the WVD in the TFPF based methods. The PWVD uses a fixed window to truncate the analyzed signal into several sections and the truncated signal in each section is regarded as linear. Nevertheless, the window length of the PWVD is fixed and does not change with the analyzed signal. Assuming we select a long window length, we suppress the random noise effectively and obtain an attenuated valid signal. When we select a short window length, we preserve the amplitude of the valid signal and obtain ineffective noise attenuation. It is significant to select frequency peak filtering, and applied the proposed method for seismic random noise attenuation. Time- frequency analysis methods can also be used in capture the features hidden in the noisy microseismic data (Chen, 2018).

In this paper, we investigate the seismic application based on the high-order synchrosqueezing transform, which can accurately calculate the instantaneous frequencies of the modes comprising the signal by making full use of the high order amplitude and phased approximations. Compared with the conventional time-frequency analysis methods, the proposed higher-order method not only enables to produce a highly energy-concentrated time-frequency representation for a wide variety of multicomponent signals but also to re- cover the original signal with a reasonably high precision.

In the following section, the fundamental theory for SST is first depicted in detail and the new method with high-order approximation for both amplitude and phase components is introduced. Next, the synthetic example is employed to demonstrate the outstanding performance in sharpening time-frequency representation over those of traditional time-frequency analysis methods. Finally, applications on two field data sets further illustrate the potential of the proposed method in highlighting the subsurface structural information with high precision, which facilitates the following seismic interpretation.

THEORY

Synchrosqueezing transform

The high-order synchrosqueezing transform is a new extension of the conventional synchrosqueezing techniques, which brings the improvement in term of accuracy of instantaneous frequency extraction (Pham and Meignen, 2017; Liu et al., 2016c, 2018b,a).

In the traditional synchrosqueezing techniques, an AM-FM signal is defined as:

$$f(\tau) = A(\tau)\, e^{i2\pi\phi(\tau)} \quad , \tag{1}$$

where $A(\tau)$ and $\phi(\tau)$ are respectively instantaneous amplitude and phase functions.

The STFT of signal f can be represented by using the following equation:

$$V_f^g(t,\eta) = \int f(\tau) g^*(\tau - t)\, e^{-i2\pi\eta(\tau - t)} d\tau \quad , \tag{2}$$

where g denotes the window function and g^* the complex conjugate of g. The conventional STFT-based SST is expressed as follows:

$$T_f^{g,\gamma}(t,\omega) = \frac{1}{g^*(0)} \int_{\{\eta, |V_f^g(t,\eta)| > \gamma\}} V_f^g(t,\eta)\, \delta(\omega - \omega_f(t,\eta)) d\eta \quad , \tag{3}$$

where γ is some threshold and δ stands for the Dirac distribution. $\omega_f(t, \eta)$ is the instantaneous frequency estimate at time t and frequency η:

$$\omega_f(t,\eta) = R\left\{ \frac{\partial_t V_f^g(t,\eta)}{i2\pi V_f^g(t,\eta)} \right\} \quad , \tag{4}$$

where $R\{Z\}$ denotes the real part of complex number Z, and ∂_t is the partial derivative with respect to t.

HIGH-ORDER SYNCHROSQUEEZING TRANSFORM

The high-order SST defines the instantaneous frequency by using the high order Taylor expansions of the amplitude and phase, that is to say, the Taylor expansions of signal *f* in eq. (1) can be written as:

$$f(\tau) = \exp\left(\sum_{k=0}^{N} \frac{[\log(A)]^{(k)}(t) + i2\pi\phi^{(k)}(t)}{k!}(\tau - t)^k\right), \tag{5}$$

where $Z^{(k)}(t)$ represents the *k*-th derivative of Z at time *t*.

Consequently, eq. (2) can be rewritten as:

$$\begin{aligned} V_f^g(t,\eta) &= \int f(\tau + t) g^*(\tau) e^{-i2\pi\eta\tau} d\tau \\ &= \int \exp\left(\sum_{k=0}^{N} \frac{[\log(A)]^{(k)}(t) + i2\pi\phi^{(k)}(t)}{k!}\tau^k\right) g^*(\tau) e^{-i2\pi\eta\tau} d\tau. \end{aligned} \tag{6}$$

By means of eq. (4), the local instantaneous frequency estimate $\omega_f(t,\eta)$ can be obtained as follows:

$$\begin{aligned} \omega_f(t,\eta) = \frac{[\log(A)]'}{i2\pi} + \phi'(t) \\ + \sum_{k=2}^{N} \frac{[\log(A)]^{(k)}(t) + i2\pi\phi^{(k)}(t)}{i2\pi(k-1)!} \frac{V_f^{t^{k-1}g}(t,\eta)}{V_f^g(t,\eta)}. \end{aligned} \tag{7}$$

Introducing the frequency modulation operator $q_{\eta,f}^{[k,N]}$ and defined by:

$$q_{\eta,f}^{[k,N]} = \frac{[\log(A)]^{(k)}(t) + i2\pi\phi^{(k)}(t)}{i2\pi(k-1)!}. \tag{8}$$

The *N*th-order local complex instantaneous frequency, $w_{\eta,f}^{[N]}$ at time *t* and frequency can be expressed by:

$$\omega_{\eta,f}^{[N]}(t,\eta) = \begin{cases} \omega_f(t,\eta) + \sum_{k=2}^{N} q_{\eta,f}^{[k,N]}(\eta,t)\left(-x_{k,1}(t,\eta)\right) \\ \quad V_f^g(t,\eta) \neq 0 and \partial_\eta x_{j,j-1}(t,\eta) \neq 0 \ (j \geq 2) \\ \omega_f(t,\eta) \\ \quad otherwise \end{cases} \tag{9}$$

Then the high-order SST is defined by replacing $\omega_f(t, \eta)$ by $w_{\eta,f}^{[N]}(t, \eta)$ in eq. (3):

$$T_{N,f}^{g,\gamma}(t,\omega) = \frac{1}{g^*(0)} \int_{\left\{\eta,\left|V_f^g(t,\eta)\right|>\gamma\right\}} V_f^g(t,\eta)\,\delta\left(\omega-\omega_{\eta,f}^{[N]}(t,\eta)\right)d\eta. \quad (10)$$

Finally, the original signal can be reconstructed by:

$$f(t) \approx \int_{\{\omega,|\omega-\varphi(t)|<d\}} T_{N,f}^{g,\gamma}(t,\omega)d\omega \quad , \quad (11)$$

where d is the compensation factor and $\phi(t)$ is an estimate for $\phi'(t)$.

EXAMPLES

Synthetic data

A synthetic signal (Fig. 1) characterized by strong nonlinear sinusoidal frequency is utilized to evaluate the performance of the proposed method. Fig. 2 show the time-frequency representations based on STFT, SST and the proposed method, respectively. It is obvious from Fig. 2 that STFT leads to a poorer time-frequency map due to its low resolutions in both temporal and frequency. Some smearing appears in the traditional SST time-frequency map. The relatively sharp time-frequency representation is achieved by the proposed method, which is much better than that corresponding to SST. For a better understanding of the improvements resulted from the proposed high-order method, we enlarge an area from the top row in Fig. 2 (the red rectangle) and show them in the bottom row of Fig. 2. It can clearly be observed that the energy is perfectly concentrated by the use of the high-order method in comparison with the other methods, which is more beneficial for us to extracting the instantaneous attributes.

Field data

In this section, we investigate the applicability of the proposed method for seismic time-frequency analysis. A field data set (Fig. 3) is considered, which consists of a total of 200 traces, with a sampling interval of 2 ms and 512 samples per trace. This data, analyzed previously by (Chen and Fomel, 2015) and Cheng et al. (2017), is from a land survey.

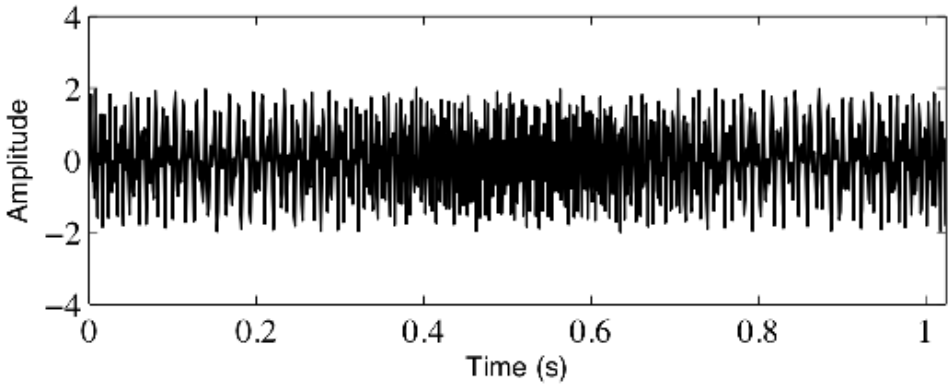

Fig. 1. Synthetic signal example.

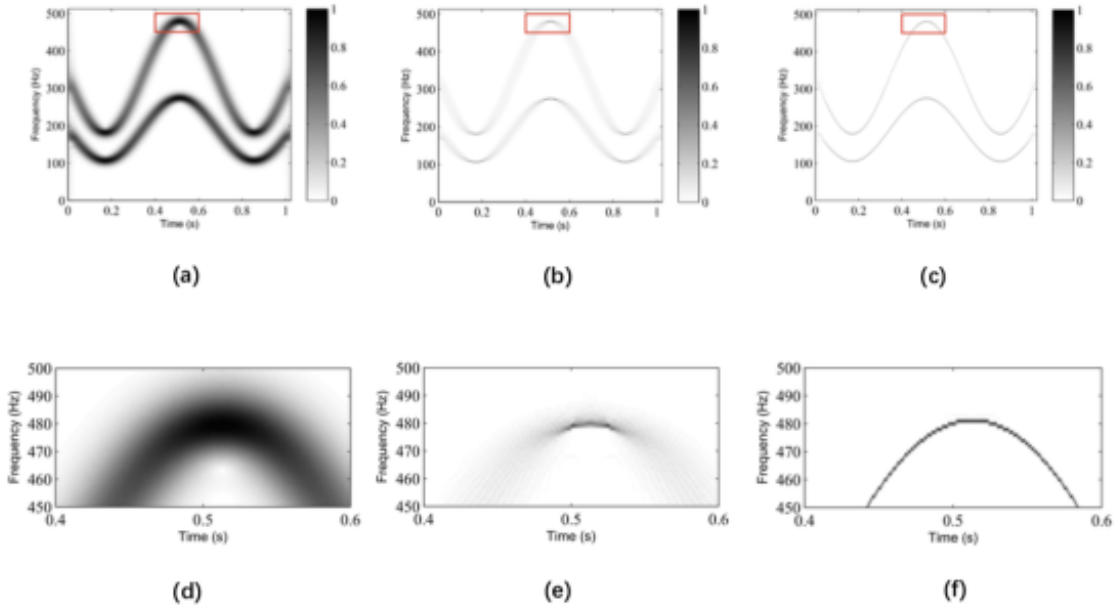

Fig. 2. Time-frequency representations. (a) Time-frequency map using STFT. (b) Time-frequency map using SST. (c) Time-frequency map using the proposed method. (d)-(f) Zoomed-in comparison of (a)-(c).

We extract the 30 Hz and 60 Hz frequency slices based on SST and the proposed methods. The results are shown in Fig. 4. The instantaneous spectrum from the two methods displays much sparer output and more distinct spectral features. However, as can be clearly seen, the SST seems to provide a set of blurred frequency slices and makes the continuity of spectrum poor, e.g., around 0.3 s and 0.4 s. In contrast, the proposed method does an excellent job in the two aspects with better continuity and much clearer results, which is very crucial in highlighting geological characteristics and extracting stratigraphic information. The two frequency slices clearly depict two low-frequency shadows, which indicates hydrocarbon reservoirs.

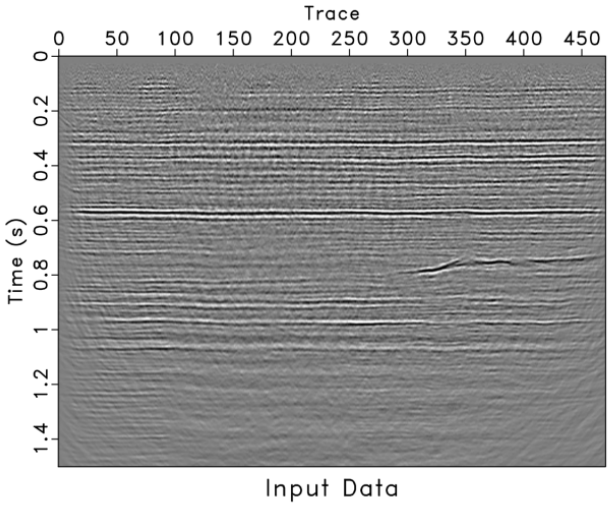

Fig. 3 Field data example for detecting low-frequency anomaly.

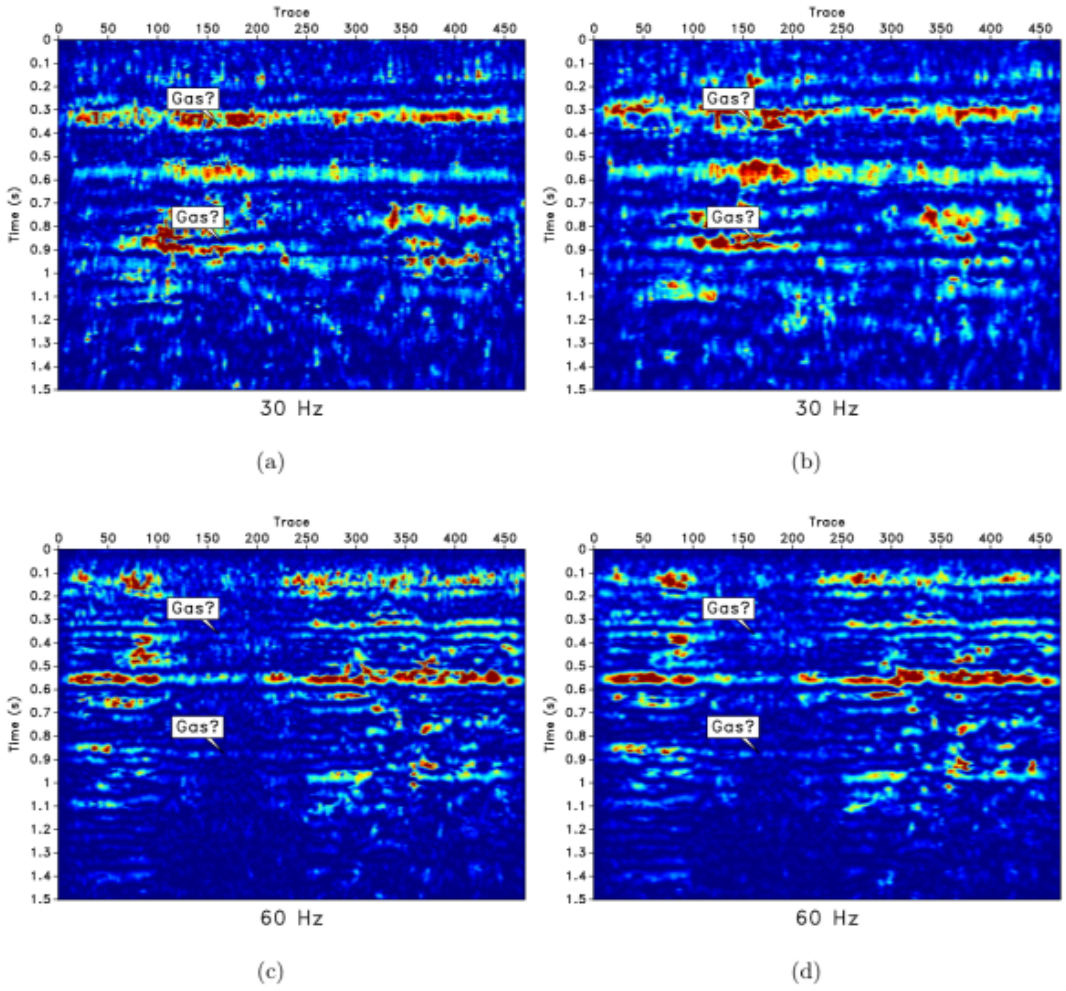

Fig. 4. Frequency slices. (a) Frequency of 30 Hz using the SST method. (b) Frequency of 30 Hz using the proposed method. (c) Frequency of 60 Hz using the SST method. (d) Frequency of 60 Hz using the proposed method.

Then, we apply the proposed time-frequency approach to a 3D data volume. It is flattened using the plane wave painting approach. The field data is from the Gulf of Mexico (Ebrahimi et al., 2017). It was previously used in Chen et al. (2017a). The constant time slice is shown in Fig. 5. From the amplitude slice, there is no obvious channel. However, after extracting different frequency slices we can observe elegant geological features, e.g., the pale-channels. Fig. 6 show four frequency slices corresponding 10Hz-40Hz using the traditional method. Fig. 7 show four frequency slices corresponding 10 Hz - 40 Hz using the proposed method. It is clear that the frequency slices from the new method has higher resolution in delineating the subsurface features, especially for the 30 Hz and 40 Hz slices. It can be seen clearly that the 30 Hz slice shows the main channel structures. The 10Hz and 20 Hz mainly show random features. When interpreting the horizon, it is better to utilize multiple frequency slices to have a more comprehensive understanding about the subsurface geological structure.

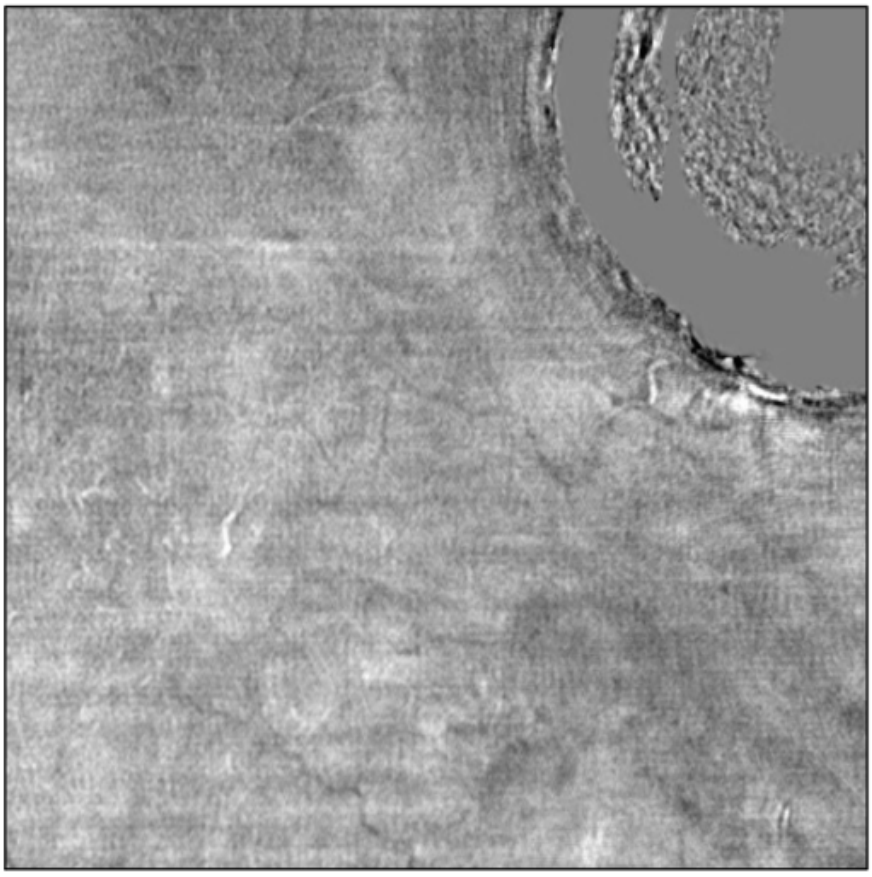

Fig. 5. Field data example for paleo-channel detection.

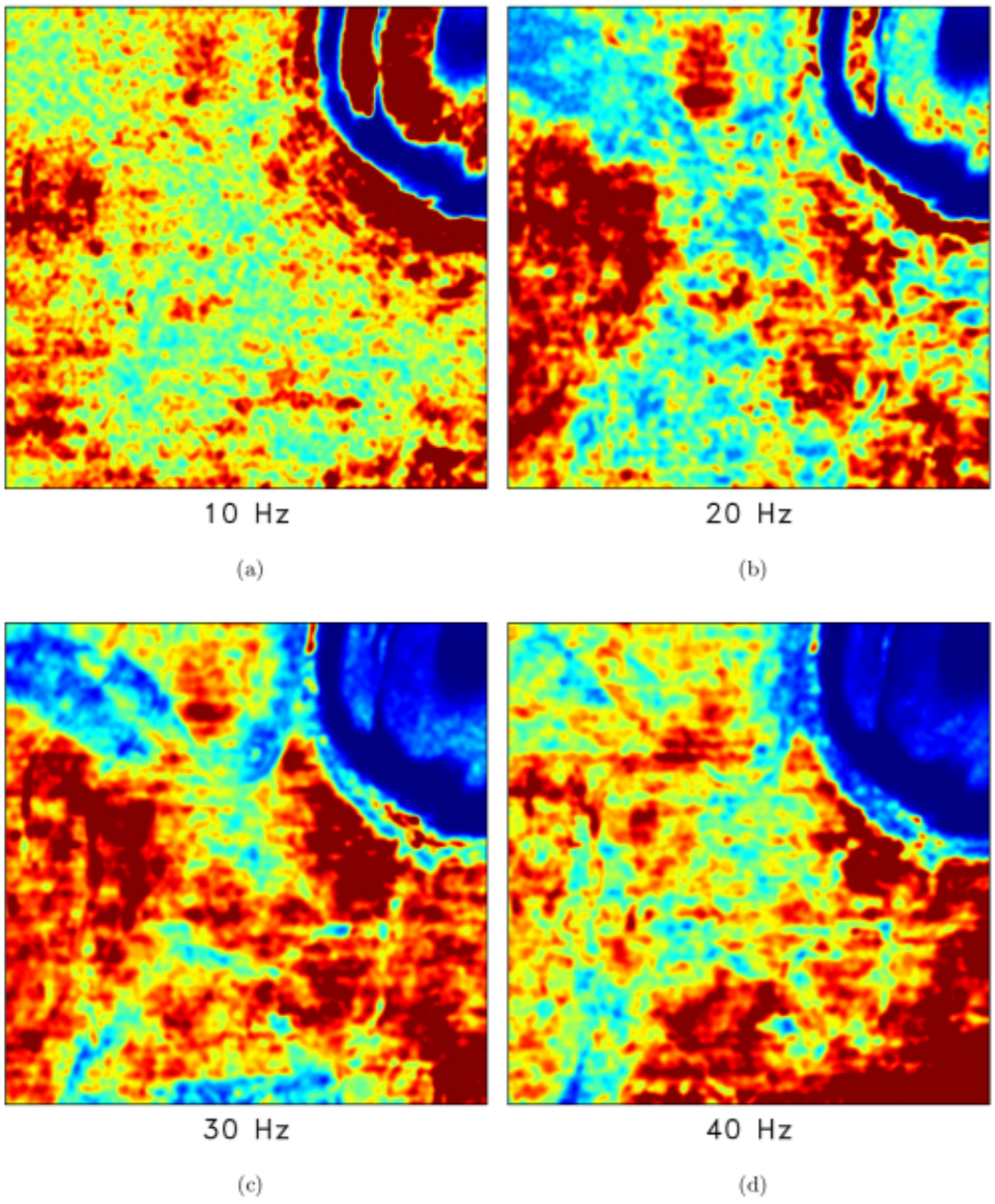

Fig. 6. Frequency slices obtained the traditional method. (a) Frequency of 10 Hz. (b) Frequency of 20 Hz. (c) Frequency of 30 Hz. (d) Frequency of 40 Hz. Note the paleo-channels highlighted in the 30 Hz slice.

CONCLUSIONS

In this paper, I have presented a novel approach for seismic time-frequency analysis and subsurface characterization. The new approach can obtain higher characterization resolution compared with the state-of-the-art algorithms. The new time-frequency analysis algorithm

defines new synchrosqueezing operators based on high approximation for both amplitude and phase in order to obtain a more energy-concentrated result. The effective- ness of the proposed method is validated by synthetic signal and field data set. The field data example demonstrate the practical applications of the proposed method detecting low-frequency shadows and paleo-channels when analyzing constant frequency slices.

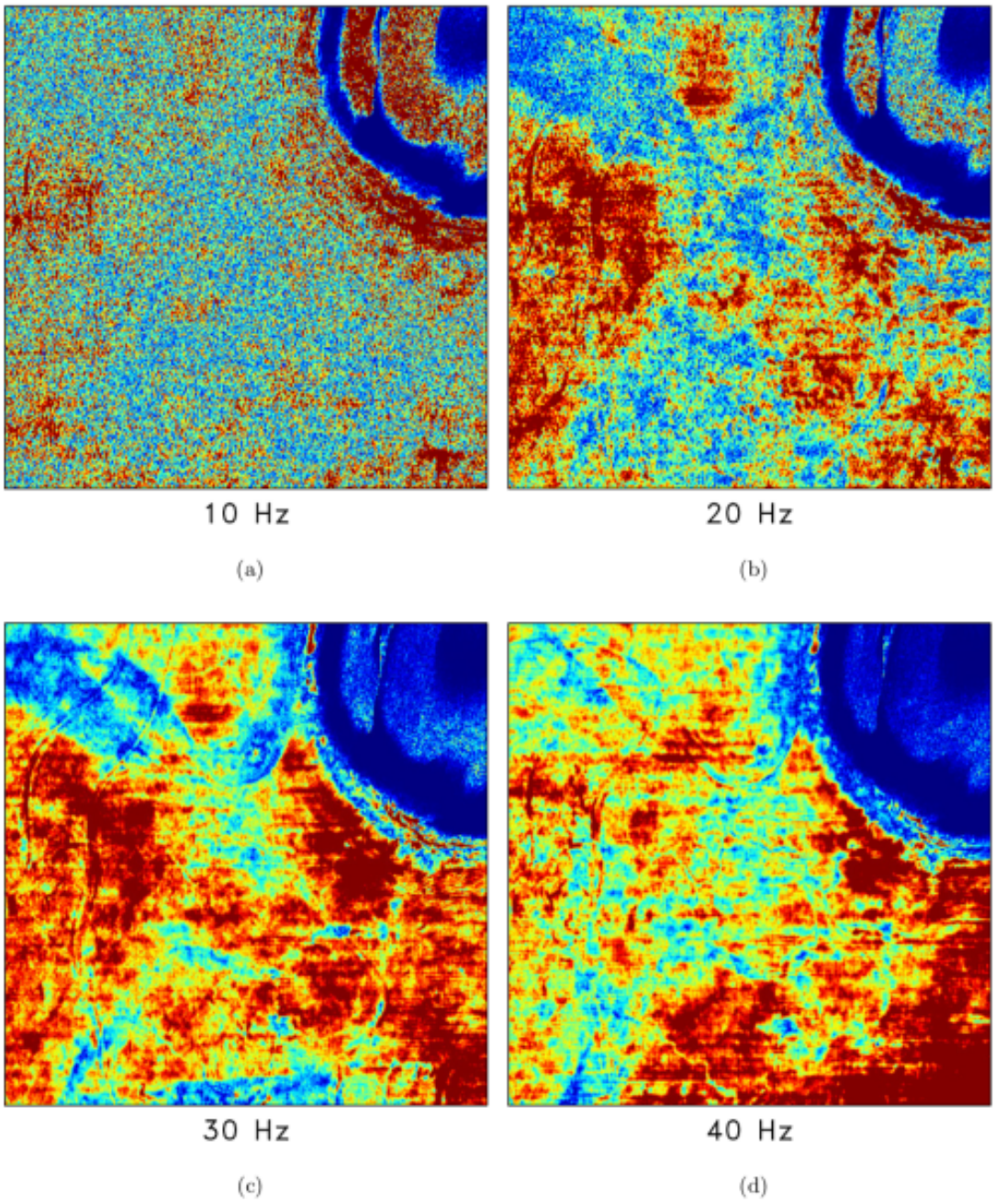

Fig. 7. Frequency slices obtained the proposed method. (a) Frequency of 10 Hz. (b) Frequency of 20 Hz. (c) Frequency of 30 Hz. (d) Frequency of 40 Hz. Note the paleo-channels highlighted in the 30 Hz slice.

REFERENCES

Allen, J.B., 1977. Short term spectral analysis, synthetic and modification by discrete Fourier transform. IEEE Transact. Acoust. Speech Sign. Process., 25: 235-238.

Castagna, J.P., Sun, S. and Siegfried, R.W., 2003. Instantaneous spectral analysis: Detection of low-frequency shadows associated with hydrocarbons. The Leading Edge, 22: 120-127.

Chen, Y., Fomel, S. and Hu, J., 2014a. Iterative deblending of simultaneous-source seismic data using seislet-domain shaping regularization. Geophysics, 79(5): V179-V189.

Chen, Y., Liu, T., Chen, X. and Li, J., 2014b. Time-frequency analysis of seismic data using synchrosqueezing wavelet transform. J. Seismic Explor., 23: 303-312.

Chen, Y. and Fomel, S., 2015. Random noise attenuation using local signal-and-noise orthogonalization. Geophysics, 80(6): WD1-WD9.

Chen, Y., 2016. Dip-separated structural filtering using seislet thresholding and adaptive empirical mode decomposition based dip filter. Geophys. J. Internat., 206: 457-469.

Chen, W., Chen, Y. and Liu, W., 2016a. Ground roll attenuation using improved complete ensemble empirical mode decomposition. J. Seismic Explor., 25: 485-495.

Chen, Y., Chen, H., Xiang, K. and Chen, X., 2016b. Geological structure guided well log Interpolation for high-fidelity full waveform inversion. Geophys. J. Internat., 207: 1313-1331.

Chen, Y., Zhang, D., Jin, Z., Chen, X., Zu, S., Huang, W. and Gan, S., 2016c. Simultaneous denoising and reconstruction of 5D seismic data via damped rank-reduction method. Geophys. J. Internat., 206: 1695-1717.

Chen, Y., 2017. Fast dictionary learning for noise attenuation of multidimensional seismic data. Geophys. J. Internat., 209: 21-31.

Chen, W., Chen, Y. and Cheng, Z., 2017a. Seismic time-frequency analysis using an improved empirical mode decomposition algorithm. J. Seismic Explor., 26: 367-380.

Chen, W., Xie, J., Zu, S., Gan, S. and Chen, Y., 2017b. Multiple reflections noise attenuation using adaptive randomized-order empirical mode decomposition. IEEE Geosci. Remote Sens. Lett., 14: 18-22.

Chen, W., Yuan, J., Chen, Y. and Gan, S., 2017c. Preparing the initial model for iterative deblending by median filtering. J. Seismic Explor., 26: 25-47.

Chen, W., Zhang, D. and Chen, Y., 2017d. Random noise reduction using a hybrid method based on ensemble empirical mode decomposition. J. Seismic Explor., 26: 227-249.

Chen, Y., Chen, H., Xiang, K. and Chen, X., 2017e. Preserving the discontinuities in least-squares reverse time migration of simultaneous-source data. Geophysics, 82(3): S185-S196.

Chen, Y., 2018. Fast waveform detection for microseismic imaging using unsupervised machine learning. Geophys. J. Internat., 215: 1185-1199.

Chen, Y. and Fomel, S., 2018. EMD-seislet transform. Geophysics, 83(1): A27-A32.

Chen, W. and Song, H., 2018. Automatic noise attenuation based on clustering and empirical wavelet transform. J. Appl. Geophys., 159: 649-665.

Cheng, Z., Chen, W., Chen, Y., Liu, Y., Liu, W., Li, H. and Yang, R., 2017. Application of bi-Gaussian S-transform in high-resolution seismic time-frequency analysis. Interpretation, 5: SC1-SC7.

Daubechies, I., Lu, J. and Wu, H.T., 2011. Synchrosqueezed wavelet transforms: An empirical mode decomposition-like tool. Appl. Computat. Harmon. Analys., 30: 243-261.

Ebrahimi, S., Kahoo, A.R., Chen, Y. and Porsani, M.J., 2017. A high-resolution weighted AB semblance for dealing with amplitude-variation-with-offset phenomenon. Geophysics, 82(2): V85-V93.

Gan, S., Wang, S., Chen, Y., Zhang, Y. and Jin, Z., 2015. Dealiased seismic data interpolation using seislet transform with low-frequency constraint: IEEE Geosci. Remote Sens. Lett., 12, 2150–2154.

Gan, S., Wang, S., Chen, Y. and Chen, X., 2016a. Simultaneous-source separation using iterative seislet-frame thresholding. IEEE Geosci. Remote Sens. Lett., 13: 197-201.

Gan, S., Wang, S., Chen, Y., Chen, X. and Xiang, K., 2016b. Separation of simultaneous sources using a structural-oriented median filter in the flattened dimension. Comput. Geosci., 86: 46-54.

Gan, S., Wang, S., Chen, Y., Qu, S. and Zu, S., 2016c. Velocity analysis of simultaneous-source data using high-resolution semblance-coping with the strong noise. Geophys. J. Internat., 204: 768-779.

Huang, N.E., Shen, Z., Long, S.R., Wu, M.C., Shih, H.H., Zheng, Q., Yen, N.-C., Tung, C.C. and Liu, H.H., 1998. The empirical mode decomposition and the Hilbert spectrum for nonlinear and non-stationary time series analysis. Proc. Roy. Soc. London, Ser. A, 454: 903-995.

Jeffrey, C. and William, J., 1999. On the existence of discrete Wigner distributions. IEEE Sign. Process. Lett., 6(12): 304-306.

Li, H., Wang, R., Cao, S., Chen, Y. and Huang, W., 2016a. A method for low-frequency noise suppression based on mathematical morphology in microseismic monitoring. Geophysics, 81(3): V159-V167.

Li, H., Wang, R., Cao, S., Chen, Y., Tian, N. and Chen, X., 2016b. Weak signal detection using multiscale morphology in microseismic monitoring. J. Appl. Geophys., 133: 39-49.

Lin, H., Li, Y., Ma, H., Yang, B. and Dai, J., 2015. Matching-pursuit-based spatial-trace time-frequency peak filtering for seismic random noise attenuation. IEEE Geosci. Remote Sens. Lett., 12: 394-398.

Liu, Y., Li, Y., Lin, H. and Ma, H., 2013. An amplitude-preserved time-frequency peak filtering based on empirical mode decomposition for seismic random noise reduction. IEEE Geosci. Remote Sens. Lett., 112: 896-900.

Liu, W., Cao, S. and Chen, Y., 2016a. Applications of variational mode decomposition in seismic time-frequency analysis: Geophysics, 81, V365–V378.

Liu, W., Cao, S. and Chen, Y., 2016b. Seismic time-frequency analysis via empirical wavelet transform. IEEE Geosci. Remote Sens. Lett., 13: 28-32.

Liu, W., Cao, S., Gan, S., Chen, Y., Zu, S. and Jin, Z., 2016c. One-step slope estimation for dealiased seismic data reconstruction via iterative seislet thresholding. IEEE Geosci. Remote Sens. Lett., 13: 1462-1466.

Liu, W., Cao, S., Liu, Y. and Chen, Y., 2016d. Synchrosqueezing transform and its applications in seismic data analysis. J. Seismic Explor., 25: 27-44.

Liu, N., Gao, J., Jiang, X., Zhang, Z. and Wang, Q., 2017a. Seismic time-frequency analysis via stft-based concentration of frequency and time. IEEE Geosci. Remote Sens. Lett., 14: 127-131.

Liu, W., Cao, S., Wang, Z., Kong, X. and Chen, Y., 2017b. Spectral decomposition for hydrocarbon detection based on VMD and Teager-Kaiser energy. IEEE Geosci. Remote Sens. Lett., 14: 539-543.

Liu, W., Cao, S., Jin, Z., Wang, Z. and Chen, Y., 2018a. A novel hydrocarbon detection approach via high-resolution frequency-dependent avo inversion based on variational mode decomposition. IEEE Transact. Geosci. Remote Sens., 56: 2007- 2024.

Liu, W., Cao, S., Wang, Z., Jiang, K., Zhang, Q. and Chen, Y., 2018b. A novel approach for seismic time-frequency analysis based on high-order synchrosqueezing transform. IEEE Geosci. Remote Sens. Lett., 15: 1159-1163.

Oberlin, T., Meignen, S. and Perrier, V., 2015. Second-order synchrosqueezing transform or invertible reassignment? Towards ideal time-frequency representations. IEEE Transact. Sign. Process., 63: 1335-1344.

Partyka, G.A., Gridley, J.M. and Lopez, J., 1998. Interpretational applications of spectral decomposition in reservoir characterization. The Leading Edge, 18: 353-360.

Pham, D.H. and Meignen, S., 2017. High-order synchrosqueezing transform for multicomponent signals analysis - with an application to gravitational-wave signal. IEEE Transact. Sign. Process., 65: 3168-3178.

Siahsar, M.A.N., Abolghasemi, V. and Chen, Y., 2017a. Simultaneous denoising and interpolation of 2D seismic data using data-driven non-negative dictionary learning. Sign. Process., 141: 309-321.

Siahsar, M.A.N., Gholtashi, S., Kahoo, A.R., Chen, W. and Chen, Y., 2017b. Data-driven multi-task sparse dictionary learning for noise attenuation of 3D seismic data. Geophysics, 82(6): V385-V396. doi: 10.1190/geo2017–0084.1.

Siahsar, M.A.N., Gholtashi, S., Olyaei, E., Chen, W. and Chen, Y., 2017c. Simultaneous denoising and interpolation of 3D seismic data via damped data-driven optimal singular value shrinkage. IEEE Geosci. Remote Sens. Lett., 14: 1086-1090.

Sinha, S., Routh, P.S., Anno, P. and Castagna, J.P., 2005. Spectral decomposition of seismic data with continuous wavelet transform. Geophysics, 70(1): P19-P25.

Thakur, G. and Wu, H.T., 2011. Synchrosqueezing-based recovery of instantaneous frequency from nonuniform samples. SIAM J. Mathemat. Analys., 43: 2078-2095.

Wang, Y., Ma, X., Zhou, H. and Chen, Y., 2018a. L1-2 minimization for exact and stable seismic attenuation compensation. Geophys. J. Internat., 213: 1629-1646.

Wang, Y., Zhou, H., Chen, H. and Chen, Y., 2018b. Adaptive stabilization for Q-compensated reverse time migration. Geophysics, 83: S15-S32.

Zhang, Q., Mao, W., Zhou, H., Zhang, H. and Chen, Y., 2018. Hybrid-domain simultaneous-source full waveform inversion without crosstalk noise. Geophys. J. Internat., 215: 1659-1681.

Zhou, Y., Li, S., Xie, J., Zhang, D. and Chen, Y., 2017. Sparse dictionary learning for seismic noise attenuation using a fast orthogonal matching pursuit algorithm. J. Seismic Explor., 26: 433-454.

Zhou, Y., Li, S., Zhang, D. and Chen, Y., 2018. Seismic noise attenuation using an online subspace tracking algorithm. Geophys. J. Internat., 212: 1072-1097.

Zu, S., Zhou, H., Chen, Y., Qu, S., Zou, X., Chen, H. and Liu, R., 2016. A periodically varying code for improving deblending of simultaneous sources in marine acquisition. Geophysics, 81(3): V213-V225.

Zu, S., Zhou, H., Mao, W., Zhang, D., Li, C., Pan, X. and Chen, Y., 2017. Iterative deblending of simultaneous-source data using a coherency-pass shaping operator. Geophys. J. Internat., 211: 541-557.